

# Identification of a Mid-anaphase Checkpoint in Budding Yeast

Sam S. Yang, Elaine Yeh, E.D. Salmon, and Kerry Bloom

Department of Biology, University of North Carolina, Chapel Hill, North Carolina 27599-3280

**Abstract.** Activation of a facultative, dicentric chromosome provides a unique opportunity to introduce a double strand DNA break into a chromosome at mitosis. Time lapse video enhanced-differential interference contrast analysis of the cellular response upon dicentric activation reveals that the majority of cells initiates anaphase B, characterized by pole–pole separation, and pauses in mid-anaphase for 30–120 min with spindles spanning the neck of the bud before completing spindle elongation and cytokinesis. The length of the spindle at the delay point (3–4  $\mu\text{m}$ ) is not dependent on

the physical distance between the two centromeres, indicating that the arrest represents surveillance of a dicentric induced aberration. No mid-anaphase delay is observed in the absence of the *RAD9* checkpoint gene, which prevents cell cycle progression in the presence of damaged DNA. These observations reveal *RAD9*-dependent events well past the G2/M boundary and have considerable implications in understanding how chromosome integrity and the position and state of the mitotic spindle are monitored before cytokinesis.

**B**UDDING yeast has been one of the key genetic systems in defining the progression of cell cycle events. One of the major paradigms is the accumulation and destruction of cyclin–cyclin-dependent kinase complexes (Nasmyth, 1993; Murray, 1995a). By delaying or advancing the timing of cyclin–cyclin-dependent kinase activity, the cell is able to coordinate steps in cell cycle progression, as well as respond to environmentally induced damage before downstream events. Cells can delay the onset of DNA synthesis (S phase) or mitosis (M phase) after exposure to x-rays,  $\gamma$  irradiation, or ultraviolet light (Hartwell and Weinert, 1989; Weinert and Lydall, 1993; Murray, 1995b). DNA lesions are recognized by proteins engaged either in DNA processing (*Rad9*, 24, 17, and *Mec3*) or signalling (*Mec1* and *Mec2/Rad53*) (Siede et al., 1993; Allen et al., 1994; Weinert et al., 1994; Lydall and Weinert, 1995). Aberrant spindle assembly and alterations in kinetochore structure and function are also subject to surveillance mechanisms that act to delay anaphase onset (Hoyt et al., 1991; Li and Murray, 1991; Spencer and Hiter, 1992; Gorbsky and Ricketts, 1993; Li and Nicklas, 1995; Wang and Burke, 1995). These lesions are monitored, at least in budding yeast, by the *MAD1*, 2, and 3 and *BUB1*, 2, and 3 genes (Hoyt et al., 1991; Li and Murray, 1991; for review see Wells, 1996).

Relatively little information addresses cell cycle regulation and checkpoint pathways that may be critical for coordinating spindle position and disassembly with cytokinesis. Our recent results from high-resolution video enhanced-

(VE)<sup>1</sup> and digital enhanced- (DE) differential interference contrast (DIC) microscopy of living cells reveal discrete kinetic and morphological transitions during anaphase progression (Yeh et al., 1995). Most notable are the sequential fast and slow phases of spindle elongation and the morphological transition from a sausage shape to a bi-lobed nucleus that accompany these rate changes. At anaphase onset, the 1.5–2  $\mu\text{m}$  spindle spanning the preanaphase nucleus elongates rapidly through the neck of the budded cell (1.0  $\mu\text{m}/\text{min}$ ) until the spindle and nucleus achieve a length of  $\sim$ 3–4  $\mu\text{m}$  in a haploid cell. The rate of spindle elongation decreases (0.3  $\mu\text{m}/\text{min}$ ), and the nucleus converts from a sausage-shaped structure to a bi-lobed configuration and elongates until the maximal length of 10–12  $\mu\text{m}$  is reached. Similar rates and evidence for biphasic spindle elongation have been obtained from observations of spindle pole body movement in living cells, as well (Kahana et al., 1995). Chromatin separation, as seen by staining with DAPI, appears to be completed in the bi-lobed nucleus. Differential regulation of microtubule dynamics and nuclear and cytoplasmic motor proteins are likely to be involved in the regulation and translocation of the spindle during anaphase. Indeed, spindle elongation is confined primarily to the mother in cells lacking the microtubule-based motor protein dynein (*DHCl*), and spindle disassembly and cytokinesis are delayed until the nucleus traverses the neck of the budded cell (Eshel et al., 1993; Li et al., 1993; Yeh et al., 1995). The spatial consequence of division by budding is that the plane of cleavage is estab-

Please address all correspondence to Kerry Bloom, Department of Biology, University of North Carolina, Chapel Hill, NC 27599-3280. Tel.: 919-962-1182; Fax: 919-962-1625; E-mail: ksb.fordham@mhs.unc.edu

1. *Abbreviations used in this paper.* DE and VE, digital and video enhanced; DIC, differential interference contrast; FISH, fluorescent in situ hybridization.

lished well before bi-polar spindle formation. This configuration requires spindle migration through the neck before successful cell division, and the dynein mutants reflect the cellular capacity to monitor spindle and/or nuclear position.

Studies in populations of budding yeast, after activation of a facultative, dicentric chromosome are also indicative of a mid-anaphase cell cycle checkpoint which can delay progression through mitosis (Neff and Burke, 1992; Brock and Bloom, 1994). These dicentric chromosomes contain two centromeres, one of which is conditionally regulated by the *GALI* transcriptional promoter (Brock and Bloom, 1994). Transcription is repressed on glucose, and the centromere is completely functional. Growth on galactose activates the promoter, which in turn, inactivates the centromere. The conditional dicentric chromosome is stably maintained in a monocentric state by growth on galactose and becomes dicentric on glucose. Cells harboring an active, dicentric chromosome are delayed in their cell cycle transit. A third to one half of the cells in a population are large budded, with nuclear DNA spanning the neck and a short spindle bisecting the nucleus, after the switch to glucose as the sole carbon source for growth (Neff and Burke, 1992; Brock and Bloom, 1994). *p34<sup>cdc28</sup>* kinase activity is elevated in cells containing an active dicentric chromosome, compared to cells with monocentric chromosomes grown on glucose for comparable times (Neff and Burke, 1992; Brock and Bloom, 1994). The inference from these studies was that the delay preceded the decline of *p34<sup>cdc28</sup>* kinase activity, and the cells were arrested prior to the exit from mitosis.

In the present study, we have used video enhanced and digital enhanced-DIC microscopy to determine the kinetics of spindle elongation in individual cells harboring an active dicentric chromosome. Having established a framework of morphological landmarks for anaphase spindle progression in wild-type cells (Yeh et al., 1995), we have quantitated the kinetics of anaphase, spindle morphology, and spindle length, in individual cells containing active dicentric chromosomes from anaphase to cytokinesis. These studies clearly demonstrate a mid-anaphase delay which is dependent upon the *RAD9* checkpoint gene. *RAD9* has been shown previously to prevent cell cycle progression in the presence of DNA damage prior to anaphase onset (Weinert and Hartwell, 1988). Our results are indicative of a regulated progression from early anaphase to late anaphase during the later stages of mitosis.

## Materials and Methods

### Media

Yeast rich medium, YPGal and YPD, contained 2% galactose and glucose, respectively, 2% peptone, and 1% yeast extract. Yeast minimal media (SD-URA) contained 0.67% yeast nitrogen base, 2% glucose or galactose supplemented with 0.5% casamino acids, and adenine (16.5  $\mu\text{g/ml}$ ).

### Strains and Plasmids

All strains used in this study are isogenic derivatives of J178-1D (*Mat a adel met14 ura3-52 leu2-3,112 his3*). The 45-kb dicentric chromosome III strain J178#24 (*his4 $\Delta$ ::URA3 GALCEN3*) was constructed by fragment-mediated transformation of the conditional centromere at the *HIS4* locus (Hill and Bloom, 1989). The *rad9 $\Delta$*  dicentric strain was constructed by frag-

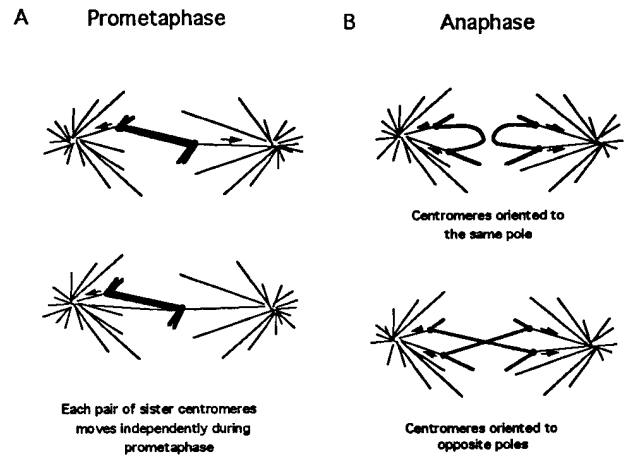


**Figure 1.** Dicentric chromosome breakage resulting from centromere movements during prometaphase or anaphase. A schematic diagram representing possible centromere attachments of a dicentric chromosome to the mitotic spindle during prometaphase and anaphase. During prometaphase, the two centromeres will independently form bipolar attachments to the mitotic spindle. A dicentric chromosome in which the two centromeres have formed initial monopolar attachments to opposite spindle poles is shown in the top figure. Centromere movements toward opposite spindle poles, as indicated by the arrows, may result in chromosome breakage. During anaphase B, when the two centromeres of a dicentric chromosome have successfully formed bipolar attachments, centromere movements at anaphase may result in chromosome breakage. If the two centromeres of each chromosome are oriented toward the same spindle pole (*top*), chromosome segregation is normal. If the centromeres are oriented toward opposite spindle poles (*bottom*), anaphase bridges are formed, and chromosome breakage can occur (Brock and Bloom, 1994).

ment-mediated transformation into J178#7 (*his4 $\Delta$ ::URA3 GALCEN3::his4*), as previously described by Brock and Bloom (1994). The 3-kb dicentric plasmid *yC<sup>2</sup>* (Hill and Bloom, 1987) was introduced into J178-1D by standard transformation. All dicentric strains were grown in galactose-containing medium to maintain chromosome III or the plasmid *yC<sup>2</sup>* as monocentric.

### Immunofluorescence

Immunofluorescent staining of yeast cells was performed essentially as described by Pringle et al. (1989). Cells were grown to early to mid-logarithmic phase growth in galactose-containing medium. Cells were pelleted, washed once with sterile water, resuspended in glucose-containing medium, and returned to 32°C for 1–2 h. Cells were fixed in 3.7% formaldehyde for 2 h at 25°C before processing for immunofluorescence. Microtubules were visualized with the rat anti- $\alpha$ -tubulin antibody YOL1/34 (Accurate Chemical and Scientific Corp., Westbury, NY). Rhodamine-conjugated goat anti-rat (Cappel Labs, Malvern, PA) was used as the secondary antibody. Cells were incubated with DAPI (1  $\mu\text{g/ml}$ ) for 5 min before the addition of mounting medium. Images were acquired and stored for further analysis, as described for FISH. Fluorescent digital images were analyzed with distance measuring tools within Metamorph software (Salmon et al., 1994).

To visualize the nucleus, cells were fixed in 3.7% formaldehyde for 1 h at 25°C. Fixed cells were washed once with water and resuspended in 1  $\mu\text{g/ml}$  DAPI for 5 min. The cells were washed once with water and mounted in mounting medium.

### Fluorescent In Situ Hybridization

J178#24 was grown to an  $A_{660} = 0.2$  density in galactose-containing medium before switching to YPD for 1 h. Cells were fixed and stained with DAPI (1  $\mu\text{g/ml}$  for 5 min) or subjected to fluorescent in situ hybridization (FISH) as described by Guacci et al. (1994). Images were visualized with a

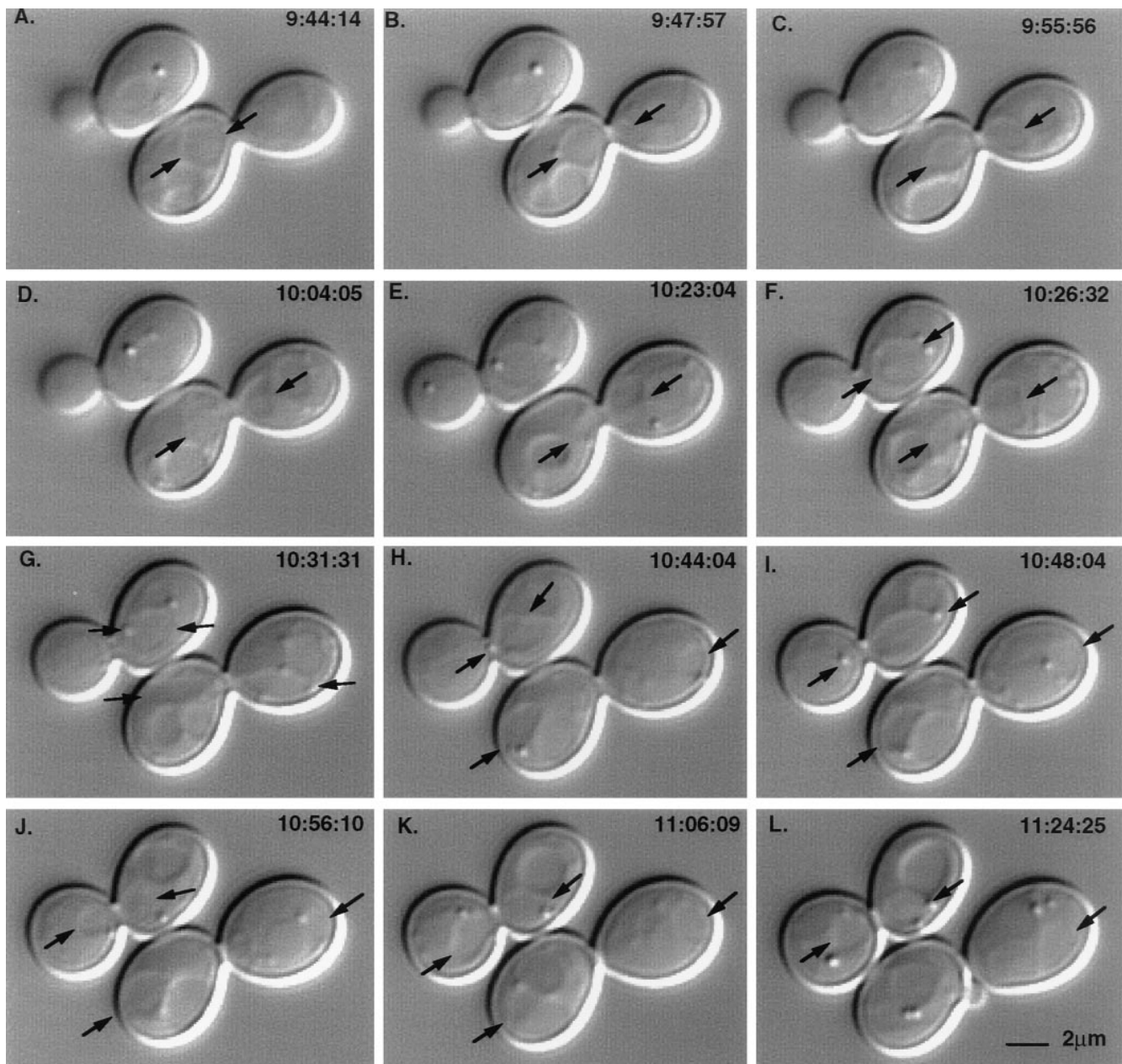


**Figure 2.** High resolution DE-DIC images of mitosis upon dicentric chromosome activation. A pair of arrows on each frame demarcates the nucleus. The time of each frame is indicated in the upper right corner. Bottom cell: (A) Pre-anaphase B/metaphase spindle (1.62  $\mu\text{m}$ ) with the nucleus positioned at the neck; (B) spindle elongation into the bud (2.99  $\mu\text{m}$ ); (C–F) the nucleus persists in the neck at a length ranging from 2.57–3.45  $\mu\text{m}$  for 38 min; (G) spindle elongation ensues (5.76  $\mu\text{m}$  spindle); (H–K) the nucleus continues to elongate to the distal ends (7.85  $\mu\text{m}$ ) and septum formation occurs (J and K); (L) cytokinesis and new bud formation. Top cell: (I) Spindle elongation; (J–K) nucleus in the neck. (L) The appearance of septum formation through the nucleus.

microscope (Microphot FXA; Nikon) using a 60X/1.4NA PlanApo objective. Metamorph software (Universal Imaging Corp., West Chester, PA) was used to control a Metaltek filter wheel (Salmon et al., 1994). A shuttered mercury lamp was used for fluorescence excitation (490 nm). Images were collected with a cooled CCD camera (C4880; Hamamatsu) and stored on an optical drive (Pinnacle Micro, Irvine, CA). 100–200 nuclei were counted.

### **Real Time Analysis of Activated Dicentric Chromosomes**

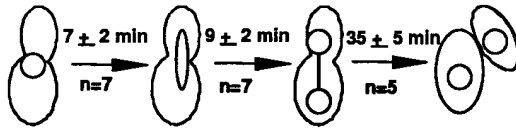
Cultures were grown to early logarithmic growth phase and spotted directly from galactose medium to YPD/25% gelatin slabs. Cells were

filmed using high resolution VE-DIC and DE-DIC microscopy and analyzed as described in Yeh et al. (1995).

### **Results**

The probability of double strand breakage in a dicentric chromosome is influenced by the behavior of each of the paired centromeres relative to the spindle poles. If the two centromeres on one sister chromatid are oriented to opposite poles, a dicentric bridge is formed, followed by breakage, or chromosome loss. Conversely, if both centromeres

### A. KINETICS



### B. SPINDLE DYNAMICS

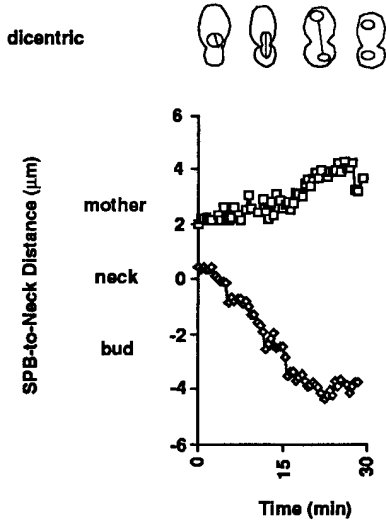


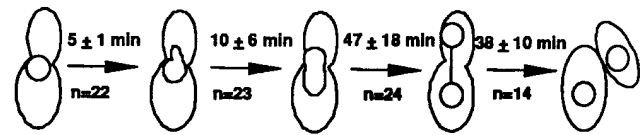
**Figure 3.** No mid-anaphase pause. (A) Kinetic analysis of changes in nuclear morphology and spindle dynamics in dicentric cells displaying wild-type kinetics. The time between spindle elongation and cytokinesis, seen as cell separation, was determined from the time lapse videos. 7 out of 29 cells filmed displayed these kinetics. (B) Spindle movements relative to the bud neck. The distance ( $\mu\text{m}$ ) between the neck and the leading and lagging edge of the nuclear envelope was measured and plotted as a function of time (min). A schematic representation of the nuclear morphology and position at the different stages is shown above the plot. The neck is designated as  $0 \mu\text{m}$ . The length from the leading edge to the neck (proximal to bud, *diamonds*) is designated with negative numbers. The length from the lagging edge to the neck (proximal to mother, *squares*) is designated with positive numbers. Preanaphase spindle is at  $T = 0$ .

from one sister are attached to the same pole, the chromosome will separate without engendering a break. If each centromere behaves independently, we expect to observe two populations of cells. Half of the cells will generate a broken chromosome, and half of the cells may propagate intact, dicentric molecules during cell division (Fig. 1; Koshland et al., 1987). The timing of decatenation of sister chromatids will also affect the behavior of the dicentric chromosome. This potential for different chromosome configurations on the spindle and hence, chromosome breakage or maintenance, has limited previous studies on populations of cells.

### Real Time Analysis of Cells Harboring an Active Dicentric Chromosome

VE-DIC microscopy of individual cells allowed us to visualize distinct cellular responses upon dicentric chromosome activation (Fig. 2). Cells containing the facultative

### A. KINETICS



### B. SPINDLE DYNAMICS

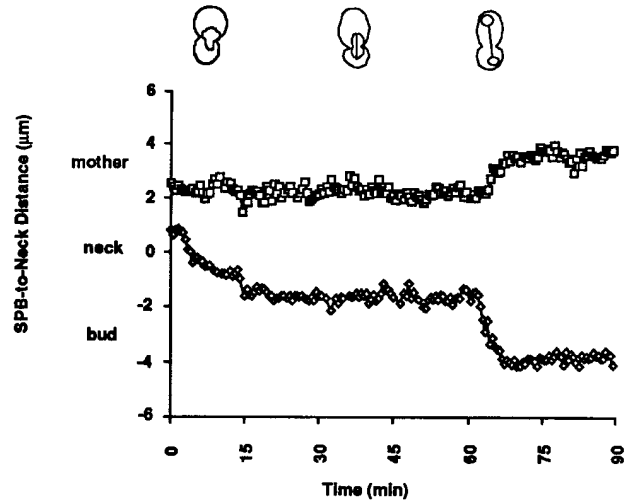


**Figure 4.** Mid-anaphase pause. (A) Kinetic analysis of changes in nuclear morphology and spindle dynamics in dicentric cells displaying mitotic delay. 22 out of 29 cells displayed these kinetics. (B) Spindle movements relative to the bud neck were determined as described in the legend to Fig. 3.

dicentric chromosome were grown to mid-logarithmic phase in galactose (monocentric conditions) and switched to glucose (dicentric conditions) for VE-DIC analysis. Two distinct mitotic populations of cells were observed (Figs. 3 and 4) and confirm the expectations predicted from the independent behavior of the two centromeres. One population, 7/29 cells (Fig. 3), mimicked wild-type cells in their kinetic progression through the cell cycle. The initial rapid elongation was completed in  $7 \pm 2$  min, the transition from the sausage shape to bi-lobed nuclear morphology took  $9 \pm 2$  min, and cytokinesis followed  $35 \pm 5$  min later (Yeh et al., 1995).

Aberrant nuclear morphology and a considerable delay between the fast and slow phases of anaphase were observed in 22/29 of the mitotic cells (Figs. 2 and 4). During the initial phases of spindle elongation, a finger-like protrusion of the nucleus into the bud was seen, rather than the typical formation of a sausage-shaped nucleus. This protrusion seemingly snaked its way into the bud for  $\sim 5 \pm 1$  min (Fig. 4 A). As the spindle elongated to  $\sim 4 \mu\text{m}$  in length, the nucleus remained rounded in shape as it traversed the neck of the dividing cell (Fig. 2 C). The time from nuclear protrusion to the formation of this rounded sausage nucleus took  $10 \pm 6$  min (Fig. 4 A). Interestingly, the nucleus continued to maintain this round to sausage-shaped morphology for  $47 \pm 18$  min before further spindle elongation and the transition to bi-lobed structures. This is significantly longer than the  $9 \pm 2$  min transition in wild-type cells, indicating a significant delay in both the kinetics

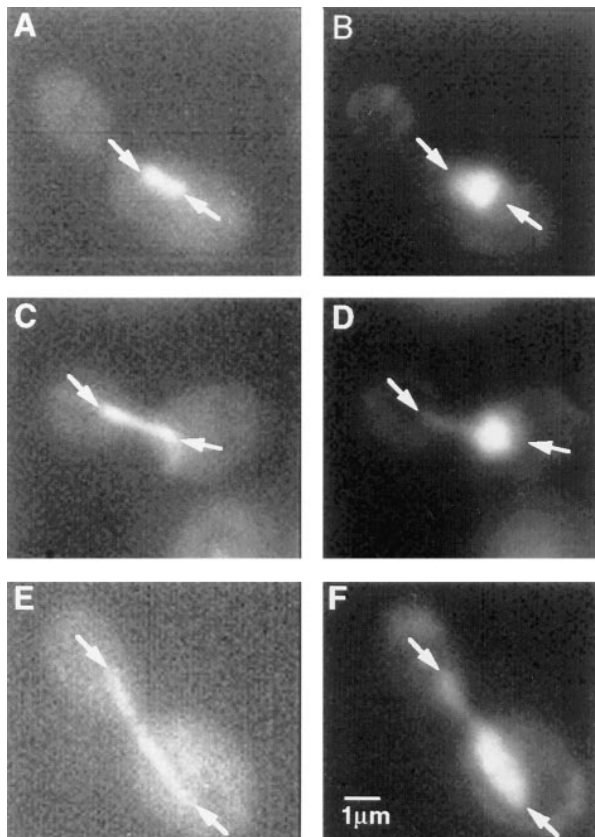


**Figure 5.** Progression of anaphase in cells containing a dicentric chromosome. Cells were fixed and processed for immunofluorescence after two hours of growth in glucose-containing medium. The panels on the left are cells stained with anti-tubulin antibodies; the panels on the right are the same cells stained with DAPI. The arrows mark the ends of the spindle or nucleus, respectively. (A and B) Cells in the G2 stage, medium budded with the DNA near the neck. (C and D) Cells in the early stages of anaphase, having a slightly elongated spindle with DNA just visible in the bud. (E and F) Typical of cells paused in mid-anaphase with a 4  $\mu\text{m}$  spindle and DNA through the neck of large budded cells. Bar, 1  $\mu\text{m}$ .

and morphological transitions that accompany anaphase B. Once the bulk of the nucleus formed a bi-lobed morphology and began the slow phase of spindle elongation, the time to cytokinesis was  $38 \pm 10$  min, similar to that observed in wild-type cells.

#### **Coincidence of Nuclear and Spindle Position at the Mid-anaphase Delay**

Bending of the mitotic spindle in and out of the plane of focus often precludes direct visualization of the spindle by VE-DIC microscopy. To confirm that position of the nucleus during mid-anaphase corresponds to actual spindle elongation through the neck, we compared the length of the nucleus in fixed cells, as determined by DAPI staining, to the length of the mitotic spindle, as visualized by indirect immunofluorescence. Cells containing the conditional dicentric chromosome were grown on galactose-containing medium and switched to glucose-containing medium for 2 h to activate the dicentric chromosome. Cells were fixed and stained for nuclear (DAPI) and spindle (anti- $\alpha$ -

tubulin immunofluorescence) analysis. In all budded cells with DNA spanning the neck (36/36), the mitotic spindle had elongated through the neck (compare Fig. 5, C and D; E and F). Quantitation of the length of tubulin immunofluorescence and of DAPI staining along the mother bud axis in G2 and mid-anaphase arrested cells shows an excellent correlation between the two measurements. In G2 cells (medium size bud, nucleus near the neck), the mean spindle length was  $1.25 \pm 0.23 \mu\text{m}$ , and the mean nuclear length was  $1.31 \pm 0.19 \mu\text{m}$  ( $n = 13$ ) (Fig. 5, A and B). Early stages of anaphase in cells containing an active dicentric chromosome were often characterized by finger-like protrusions of the nucleus into the bud (Fig. 2 B, VE-DIC; Fig. 5 D, DAPI staining). Correspondingly, the spindle spanned the distance from the end of the bulk of chromatin in the mother to the tip of the finger-like protrusion in the bud (Fig. 5 C, 2.54  $\mu\text{m}$  in length). In cells exhibiting a mid-anaphase pause, the mean spindle length was  $4.17 \pm 0.92 \mu\text{m}$  and the mean nuclear length was  $4.09 \pm 0.91 \mu\text{m}$  (Fig. 5, E and F,  $n = 31$ ). Thus the fixed images corroborate the progression, as well as the length measurements, in early to mid-anaphase, as determined in the real time analysis, and indicate the close correspondence between nuclear and spindle elongation throughout anaphase.






#### **Kinetic Analysis of Spindle Elongation**

The kinetics of spindle elongation were determined using a semi-automated tracking system to quantitate spindle morphogenesis and elongation (Skibbens et al., 1993). The direction of spindle movement could be assessed by determining the position of the leading and lagging edge of the nuclear envelope relative to the neck of the budded cell. The neck provided an accurate frame of reference in standardizing data from individual cells and was set at 0  $\mu\text{m}$ . Movements of the spindle pole into the bud (leading edge) were plotted as negative values and movement into the mother (lagging edge) as positive values. The nucleus abutted the neck immediately preceding spindle elongation, and elongation was directed into the bud. In an example of a dicentric cell that displayed wild-type kinetics, both fast and slow phases of spindle elongation, from 2 to 8–10  $\mu\text{m}$ , were complete in  $\sim 22$  min (Fig. 3 B). Cells delayed in anaphase B progression (Fig. 4 B) displayed the initial rapid elongation phase (2–4  $\mu\text{m}$ ), which was followed by a pause in spindle elongation in which the nucleus remained in the neck for a significant amount of time (up to 60 min in Fig. 4 B). Only after this pause, was the second phase of elongation able to proceed to the maximal spindle length of 10–12  $\mu\text{m}$ .

#### **Sister Chromatid Separation at the Mid-anaphase Transition**

The partially elongated spindles indicate a delay in anaphase B spindle pole separation. However, the degree of chromosome separation was not apparent in the VE-DIC images. We therefore used FISH to visualize sister chromatids in cells arrested in mid-anaphase. Asynchronous populations of cells containing the conditional dicentric chromosome were grown on galactose and switched to glucose for 1–2 h, when  $\sim 16\%$  of the cells were arrested as large budded cells with DNA spanning the neck (Table I).

Table I. Quantification of Nuclear Morphology by DAPI

					
J178-1D (No dicentric)	48%	31%	14%	4%	3%
J178-1D #7 Gal (Inactive dicentric)	39%	33%	10%	4%	14%
J178-1D #7 Glu (Active dicentric)	37%	25%	12%	16%	10%

Cells were grown to early- to mid-logarithmic phase growth in galactose media and switched to glucose media for 2 h before fixing and staining with DAPI. The position of the DNA was determined by fluorescence microscopy. >200 cells were counted.

Using chromosomal markers proximal to CEN1 on chromosome I (kindly provided by V. Guacci; Guacci et al., 1994), we determined that 34% of cells containing an active dicentric chromosome contained two spots within the nucleus (Fig. 6). In contrast, 8% of the cells were observed to have two fluorescent spots within the nucleus in wild-type, asynchronous populations using the same DNA probes (Fig. 6). The 8% of cells with separated sisters in wild-type populations can be attributed to the time expected for centromeres to separate within one chromatin mass (Yeh et al., 1995). Anaphase spindle elongation (from the fast phase to the bi-lobed structures) persists for ~9 min (Fig. 3 A). 9/90 min doubling time predicts that 10% of the population will be caught in the mid-anaphase stage. This value compares quite favorably to the 8% determined by FISH (Fig. 6 B; Guacci et al., 1994). By the same reasoning we can predict what fraction of cells harboring a dicentric chromosome will be in mid-anaphase in a logarithmic growing population. The dicentric delay persists for 57 min (Fig. 4). The doubling time of this population is ~150 min, resulting in ~38% of the cells at the mid-

anaphase transition at any one time. However, only about a third of the cells in a population pause in response to activation of the dicentric chromosome (Neff and Burke, 1992; Brock and Bloom, 1994). We therefore estimate  $2/3(8\%) + 1/3(38\%) = 17.8\%$  of cells to be in mid-anaphase. This value compares quite favorably to the 16% of cells found to be in mid-anaphase, as determined by DAPI staining (Table I), but less than that determined by FISH (34%). While the high FISH value is certainly indicative of sister chromatid separation in the population of mid-anaphase cells, it may also reflect centromere separation in a fraction of large-budded cells with DNA at the neck (Table I) as well as cells with separated nuclei (Table I, last column), in which the spindles may have collapsed and given rise to apparently undivided nuclei with two spots. In any case, the centromere regions of sister chromatids have separated in nuclei of cells containing active dicentric chromosomes, indicating these cells traverse the metaphase/anaphase boundary and become blocked following either anaphase A or anaphase A and B, with partially elongated spindles, i.e., mid-anaphase.

### Checkpoint Versus Physical Constraints on Spindle Elongation

The mid-anaphase delay could reflect a physical constraint on spindle elongation, with the DNA between the two centromeres constraining the poles from further separation. Alternatively, a cellular response to the dicentric insult could prevent further elongation (Fig. 7). To distinguish between these possibilities we have analyzed the kinetics and spindle length of the mid-anaphase transition in cells containing variants of dicentric chromosome III, in which the centromeres are 3 vs. 45 kb pairs apart. 45 kb of DNA is ~15  $\mu\text{m}$  in its linear form. Estimation of the packing ratio in chromatin (sevenfold around a nucleosome) or the degree of condensation from FISH (80 fold; Guacci et al., 1994) provide an approximate length of this region to be anywhere from 0.2–2  $\mu\text{m}$  in vivo. Similarly, dicentric chro-

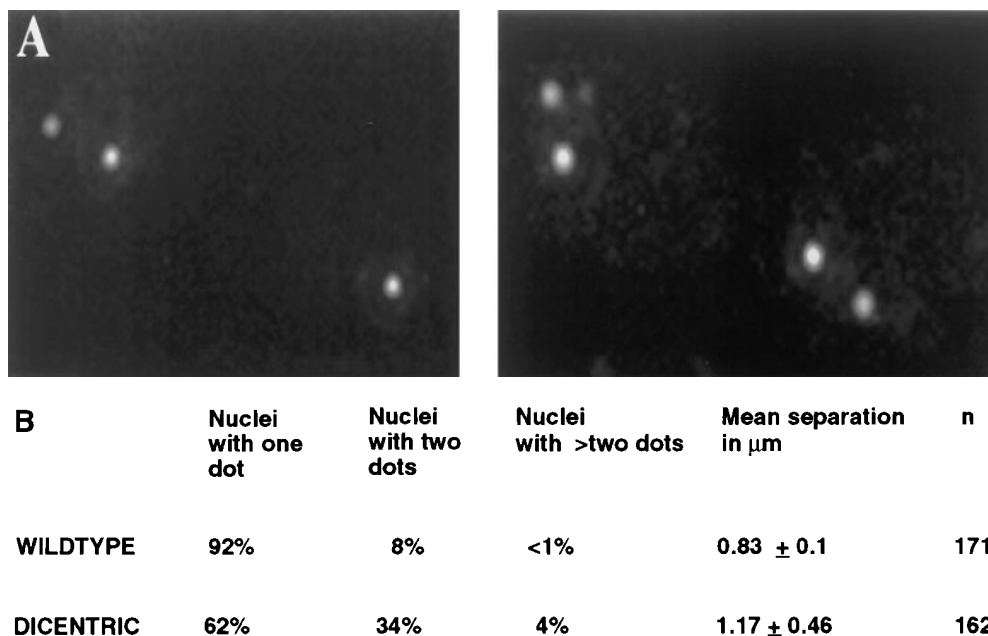


Figure 6. Quantitation of sister chromatid separation by FISH. Cells were exposed to glucose for 1 h and subjected to FISH analysis, as described in the *Materials and Methods*. (A) Micrographs of nuclei are shown. Chromosomal DNA, stained with propidium iodide, appears gray. Centromere-proximal chromosomes I are detected by FISH and appear as white dots. (B) The percentage of nuclei with one, two, or three signals was determined. Mean separation between two dots was determined.

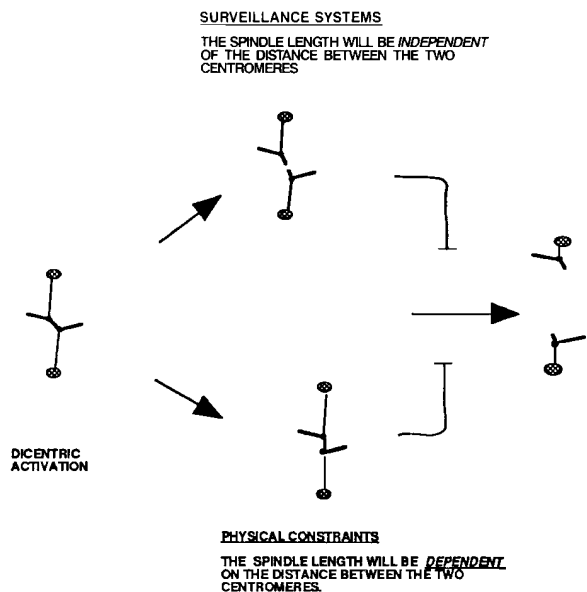


Figure 7. Nature of the mid-anaphase pause. The arrest in mid-anaphase B may be due to physical constraints on the chromosome during spindle elongation. This would predict a dependent relationship between spindle length and the distance between the two centromeres. Alternatively, activation of the dicentric chromosome and subsequent chromosomal alterations may signal a surveillance system resulting in cell cycle arrest. Spindle length at the mid-anaphase transition would be independent of the distance between the two centromeres.

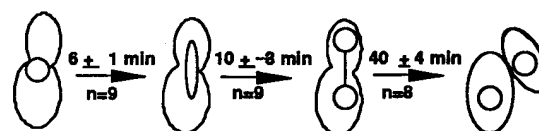
mosomes with their centromeres 3 kb apart would be expected to span  $\sim 0.02\text{--}0.2\ \mu\text{m}$  in vivo. If the physical constraint model is correct, the length of the spindle at the arrest point would reflect centromere-centromere distances, and activation of a dicentric chromosome with the centromeres 3 kb apart might result in a 10-fold difference in spindle length at the delay point. As shown in Fig. 8, cells containing the 3-kb dicentric minichromosome exhibit similar kinetics and morphologies as those of a cell containing the 45-kb dicentric chromosome. Thus the mid-anaphase pause is not a function of the length between the two centromeres.

### Checkpoint Genes in the Mid-anaphase Transition

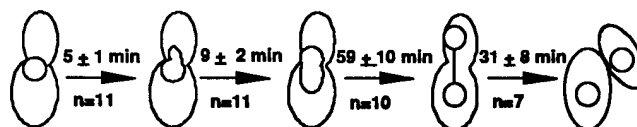
Defects in chromosome alignment, kinetochore attachment, or DNA breakage have all been shown to be subject to cell cycle surveillance. The distinguishing feature of defects monitored by these checkpoint pathways is that they delay anaphase onset. Previous studies performed by DAPI staining of fixed populations and FACS<sup>®</sup> analysis have revealed *RAD9* to be involved in mediating the dicentric response (Brock and Bloom, 1994). We have reexamined the role of *RAD9* in the real time assay to determine whether the delay in mid-anaphase is also dependent upon this checkpoint gene. A single cellular response was observed upon dicentric chromosome activation in the *rad9* deletion strain (Fig. 9, 9/9 cells; Table II). The behavior of the spindle and the timing of nuclear transitions were indistinguishable from wild-type cells.

### A. KINETICS

#### NO MID-ANAPHASE PAUSE



#### MID-ANAPHASE PAUSE



### B. SPINDLE DYNAMICS OF MID-ANAPHASE PAUSE

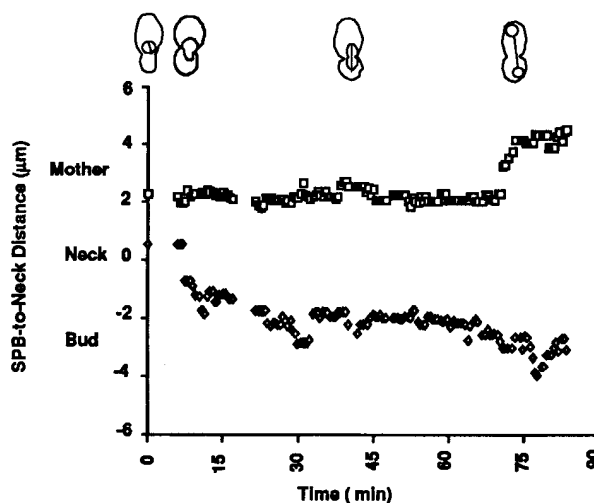


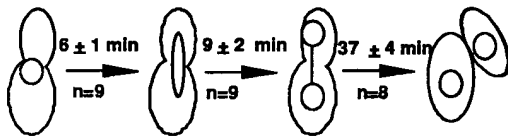
Figure 8. Kinetics and spindle dynamics upon activation of a dicentric minichromosome. The distance between the two centromeres is 3 kb. As shown in Figs. 3 and 4, two cellular responses are observed upon dicentric activation. (A) No mid-anaphase pause: Approximately 50% of the cells (9/19) exhibit wild type kinetics. Mid-anaphase pause: The other 50% (11/19) are delayed in the 3–4  $\mu\text{m}$  stage of spindle elongation (finger projection, gourd-shaped nucleus). The average time spent in mid-anaphase was  $59 \pm 10$  min. (B) The distance ( $\mu\text{m}$ ) between the neck and the leading edge of the nucleus was determined as a function of time (min). A schematic representation of the nuclear morphology and position at the different stages is shown above each plot. 0, neck; positive values, mother; negative values, bud.

### Discussion

Time lapse, VE- and DE-DIC analysis of cells containing an active dicentric chromosome reveals a delay in their progression through anaphase. By two criteria, spindle elongation and sister chromatid separation, cells containing an active dicentric chromosome transiently pause in mid-anaphase, before maximal spindle elongation and the exit from mitosis. This mid-anaphase delay is dependent on the *RAD9* DNA checkpoint gene, indicative of DNA damage surveillance pathways operative during late stages in the cell cycle (Fig. 10).

The mid-anaphase delay was distinguished by both kinetic and morphological criteria. Upon activation of the dicentric chromosome, the bulk of the nucleus remained in

## A. KINETICS



## B. SPINDLE DYNAMICS

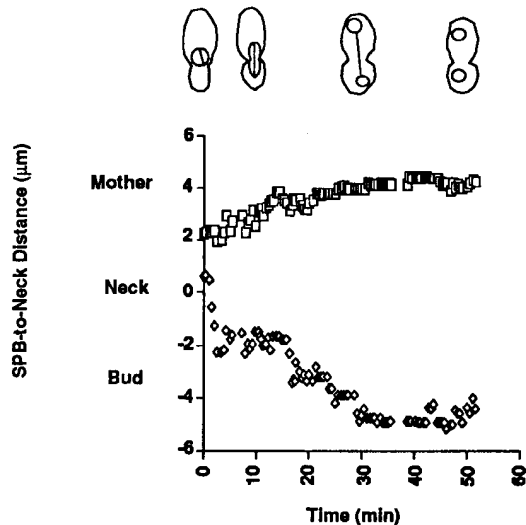


**Figure 9.** The dicentric chromosome-induced mid-anaphase transition is dependent upon the *RAD9* gene. A single cellular response was observed upon dicentric chromosome activation in the *rad9* deletion strain. The behavior of the spindle and the timing of nuclear transitions were indistinguishable from wild type cells. (A) Kinetics of morphological transitions. (B) The distance between the neck and each spindle pole body was determined as a function of time (min). A schematic representation of the nuclear morphology and position at the different stages is shown above each plot. 0, neck; positive values, mother; negative values, bud. Spindle elongation is complete after 30 min with virtually no delay in spindle elongation at the 3–4  $\mu\text{m}$  stage.

the mother cell as the spindle began to elongate (Fig. 2 B). Even as the spindle doubled its length the nucleus remained rounded and only later became noticeably sausage shaped (Fig. 2 C). In contrast, the nucleus in wild-type cells underwent a rounded to sausage-shaped transition as it traversed the neck and elongated to 4  $\mu\text{m}$  (Fig. 3; Yeh et al., 1995). The morphological transitions characteristic of dicentric chromosome activation were accompanied by a 30–120-min temporal delay in the subsequent elongation of the mid-anaphase spindle. This 4  $\mu\text{m}$  stage of spindle morphogenesis is likely to represent a critical juncture in spindle function in wild-type cells as well. In an elegant three-dimensional, serial section reconstruction of a yeast spindle, populations of anaphase spindles sorted into two classes based on their lengths: 3.7 and 9.4  $\mu\text{m}$  (Winey et al., 1995). Both populations of spindles were shown to straddle the neck, and in either population, sister chromatids had already migrated to the poles based upon the length of the presumptive kinetochore microtubules. These data corroborate our findings that sister chromatids have separated at the 4  $\mu\text{m}$  mid-anaphase delay (Fig. 6). The pre-

**Table II.** Anaphase B Dicentric Pause Is Dependent on *RAD9*

Relevant genotype	Distance between centromeres	Time of delay	Spindle length	n
<i>his4::GALCEN RAD9</i>	45 kb	47 $\pm$ 18 min	4 $\mu\text{m}$	24
<i>pYC<sup>2</sup> RAD9</i>	3 kb	51 $\pm$ 33 min	4 $\mu\text{m}$	9
<i>his4::GALCEN rad9</i>	45 kb	No delay	n.a.*	9

\*n.a., not applicable.

ponderance of 3.7  $\mu\text{m}$  spindles reported by Winey et al. (1995) also reflects the brief pause which often occurs in wild-type cells between the fast and slow phases of anaphase spindle elongation (Yeh et al., 1995). In addition, the oscillatory motion observed in the 4  $\mu\text{m}$  spindle in wild-type cells (Yeh et al., 1995) is indicative of a natural transition in spindle progression. Thus, both serial reconstruction of fixed cells and VE-DIC microscopy of live preparations indicate a clear transition from medial to elongated nuclear structures in wild-type cells. The dicentric chromosome insult simply prolongs this natural transition in the development of the anaphase spindle.

There are several aspects of dicentric chromosome activation that may contribute to the delay. One is that tension generated by the chromosome bridge could restrain spindle elongation. The finger-like protrusions of the nucleus into the bud (Figs. 4 A and 5 D), appear to be futile attempts by the spindle/nucleus to initiate anaphase spindle pole separation. This period (5 min duration) has no correlate in the kinetic progression of a wild type cell. These protrusions, and the rounded morphology of the nucleus as it traversed the neck of the dividing cell (Fig. 2 C), probably reflect transient physical constraints on the spindle. The time lapse studies with centromeres at different distances (3 vs. 45 kb apart) indicate that the arrest in spindle elongation is not exclusively due to a DNA bridge constraining anaphase pole separation. Cells containing either dicentric chromosome display virtually identical spindle morphologies and lengths (4  $\mu\text{m}$ ) for similar durations (47–59 min on average; Table II). Thus the mid-anaphase delay likely represents surveillance mechanisms that effectively inactivate the microtubule assembly and motility mechanisms which normally produce further spindle elongation.

The dependency of the mid-anaphase delay on the *RAD9* gene reveals that the DNA damage checkpoint continues to monitor chromosome integrity well after the start of anaphase, as well as before anaphase onset (Fig. 10). Thus *RAD9*-dependent DNA damage arrests the cell at any stage (G1, S, G2, and now mid-anaphase). This notion is similar to recent findings that checkpoint genes (*RAD9*, Siede et al., 1993; and the *SADI/RAD53* protein kinase, Allen et al., 1994) indeed control multiple checkpoints. Whether the damage leads to the same or different signal in each stage, or different signals in the same stage, is not well understood, but several genes are clearly involved at multiple stages of the cycle. Rad9p is constitutively expressed throughout the cell cycle (Schiestl et al., 1989), consistent with the proposal that this protein is involved in DNA surveillance throughout G1/S, G2/M, and anaphase/cytokinesis. It is also likely that DNA lesions, in addition to a dicentric-induced aberration, are also subject to *RAD9* surveillance at mid-anaphase. However, due to the



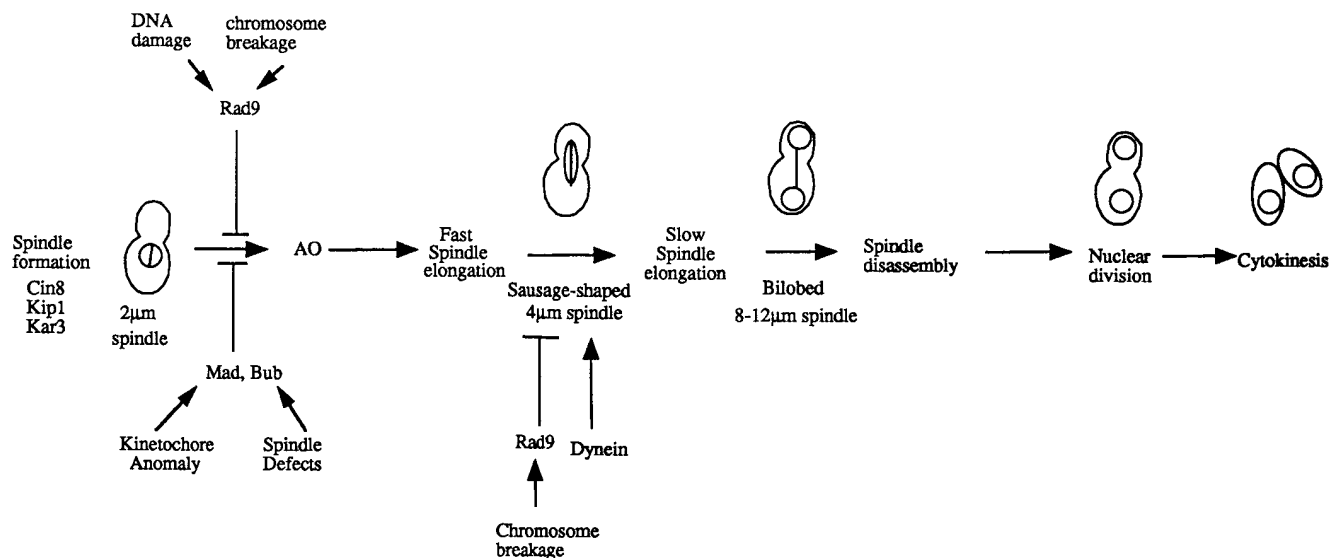


**Figure 10.** Anaphase spindle morphogenesis in yeast. The major transitions in spindle morphogenesis. Formation and maintenance of a 2  $\mu\text{m}$  spindle are dependent upon members of the kinesin family (*CIN8*, *KIP1* and *KAR3*; Saunders and Hoyt, 1992; Saunders et al., 1995), and checkpoint genes that limit anaphase onset (*AO*)(*BUB1*, 2, and 3, Hoyt et al., 1991; *MAD1*, 2 and 3, Li and Murray, 1991; *RAD9*, Weinert and Hartwell, 1988). Separation of the spindle poles (spindle elongation) and translocation of the spindle through the bud neck are simultaneous in wild type cells, characterized by fast spindle elongation (Yeh et al., 1995). VE-DIC microscopy of live cells and of serial reconstruction of yeast spindles indicates a transition between the fast (1  $\mu\text{m}/\text{min}$ ) to slow (0.3  $\mu\text{m}/\text{min}$ ) phases of spindle morphogenesis in wild type cells. This transition in mid-anaphase is prolonged upon activation of the dicentric chromosome and is dependent upon *RAD9* function. Chromosome separation (noted morphologically by the bilobed structure) is delayed upon activation of the dicentric chromosome. The final stages of spindle elongation, disassembly, nuclear division, and cytokinesis are discrete morphological events (Copeland and Snyder, 1993; Yeh et al., 1995). We propose that this mid-anaphase checkpoint is essential for coordinating spindle morphogenesis and position with chromosome separation and the onset of cytokinesis.

rapidity of spindle elongation and the relatively extended lengths of G1/S and G2/M, the mid-anaphase delay would be difficult to identify in a population study. In this regard, we have examined the effect of a dominant negative form of topoisomerase I (*top1-103*), which also results in a *RAD9*-dependent cell cycle arrest (Levin et al., 1993). As reported previously, a large fraction of cells exhibited the large budded *RAD9*-dependent arrest morphology following 8 h of *top1-103* induction. However, DAPI staining of the cells revealed two classes of arrest morphologies. About two-thirds of the cells displayed a single nucleus at the neck of large budded cells, while one-third exhibited elongated nuclei (sausage-shaped) spanning the neck region between the mother and bud (Beach, D., and K. Bloom, unpublished results). This second class of cells is identical in morphology to cells which arrest in mid-anaphase and indicates that a variety of DNA lesions can lead to delays in mid-anaphase.

The description of a mid to late-anaphase checkpoint leads to the notion that the major cyclin-dependent kinase-cyclin complexes, other regulatory kinases, e.g., *DBF2* and *20* (Toyn and Johnston, 1994), cyclin destruction, or other anaphase-progression factors, are operative after anaphase onset (Irniger et al., 1995). In fact, H1 kinase levels remain elevated for prolonged periods in yeast cell populations following activation of the dicentric chromosome (Neff and Burke, 1992; Brock and Bloom, 1994). Cyclins and H1 kinase activity persist throughout anaphase in budding yeast, *Drosophila*, and nontransformed mammalian cells (Surana et al., 1993; Girard et al., 1995; Sigrist et al.,

1995). In budding yeast, fully activated cyclins or overexpression of nondegradable forms of cyclin prevent spindle disassembly at telophase, rather than anaphase onset (Stueland et al., 1993; Surana et al., 1993), and high levels of *cdc28/clb* are found in cells arrested at telophase (*cdc15*; Surana et al., 1993; Irniger et al., 1995). The persistence of cyclin/*clb* complexes throughout anaphase raises the possibility that they may be involved in regulating the progression of anaphase directly, or by delaying anaphase progression in response to perturbation. The coexistence of subpopulations of degraded and protected cyclins (Irniger et al., 1995) is also suggestive of a role for the *cdc28/cyclin B* complex in mediating the progression of anaphase, spindle disassembly, and cytokinesis. Thus the sequential degradation of different cyclins may drive the progression from metaphase to telophase, or may be required to delay anaphase progression in the event of damage.

The description of a mid-anaphase transition raises two major questions. Upon sister chromatid separation, the cells lose a major pathway for repair of DNA damage. Therefore, why have a mid-anaphase checkpoint? Secondly, what perturbations are monitored by this checkpoint in the normal course of cell division? Several attributes of mitosis in budding yeast shed light on these issues. Yeast chromosomes have not been observed to align on a metaphase plate before anaphase onset. This has been thought to reflect the absence of chromosome condensation. However, Winey et al. (1995) demonstrated that kinetochore microtubules shorten asynchronously, reflecting the asynchronous movement of chromosomes to

the poles. Mid-anaphase may therefore represent the last time in the cell cycle where errors in attachment may be rectified. Alternatively, the mid-anaphase transition could represent the last stage for DNA repair between sister chromatids. While FISH experiments (Guacci et al., 1994) and results from analysis of sister chromatids at the mid-anaphase delay (Fig. 6) indicate that sister centromeres have separated at this stage, the chromosome arms may not be completely disjoined. The uniformity of DAPI staining in cells with 4  $\mu\text{m}$  spindles spanning the neck indicates that the bulk of the chromosomal DNA is evenly distributed within the nucleus. In contrast, the morphological transition to a bi-lobed nucleus results in substantial separation of chromosomal DNA. This most likely represents the final decatenation between sister chromatids and the irreversible commitment to chromosome separation (Fig. 10). In this view, the mid-anaphase transition represents the stage prior to the final commitment to complete DNA separation. The temporal coordination between completion of sister chromatid decatenation and force generation for spindle elongation necessary for preventing chromosome breakage may be the primary reason for the mid-anaphase pause, and one that may be important for all eukaryotic organisms. Loss of coordination of these events in transformed cells lacking mid-anaphase checkpoints may result in increased chromosome breakage, giving rise to chromosomal rearrangements, loss of genomic integrity, and hence, the neoplastic state.

We thank Dr. Vinny Guacci (Carnegie Institute, Baltimore, MD) for his generous gifts of probes, protocol, and invaluable expertise for the FISH experiments. We thank Drs. Danny Lew (Duke University, Durham, NC) and Jim Allen (University of North Carolina, Chapel Hill, NC) for critical comments. Thank you also to Paul Maddox for assistance with microscopy and image processing.

This work was supported by research grants from the National Institutes of Health General Medical Sciences (K. Bloom and E.D. Salmon).

Received for publication 6 June 1996 and in revised form 15 November 1996.

## References

- Allen, J.B., Z. Zhou, W. Siede, E.C. Friedberg, and S.J. Elledge. 1994. The SAD1/RAD53 protein kinase controls multiple checkpoints and DNA damage-induced transcription in yeast. *Genes Dev.* 8:2401–2415.
- Brock, J.A., and K. Bloom. 1994. A chromosome breakage assay to monitor mitotic forces in budding yeast. *J. Cell Sci.* 107:891–902.
- Copeland, C.S., and M. Snyder. 1993. Nuclear pore complex antigens delineate nuclear envelope dynamics in vegetative and conjugating *Saccharomyces cerevisiae*. *Yeast* 9:235–249.
- Eshel, D., L.A. Urrestarazu, S. Vissers, J.C. Jauniaux, J.C. van Vliet-Reedijk, R.J. Planta, and I.R. Gibbons. 1993. Cytoplasmic dynein is required for normal nuclear segregation in yeast. *Proc. Natl. Acad. Sci. USA.* 90:11172–11176.
- Girard, F., A. Fernandez, and N. Lamb. 1995. Delayed cyclin A and B1 degradation in non-transformed mammalian cells. *J. Cell Sci.* 108:2599–2608.
- Gorbisky, G.J., and W.A. Ricketts. 1993. Differential expression of a phosphoepitope at the kinetochores of moving chromosomes. *J. Cell Biol.* 122:1311–1321.
- Guacci, V., E. Hogan, and D. Koshland. 1994. Chromosome condensation and sister chromatid pairing in budding yeast. *J. Cell Biol.* 125:517–530.
- Hartwell, L.H., and T.A. Weinert. 1989. Checkpoints: controls that ensure the order of cell cycle events. *Science (Wash. DC)* 246:629–634.
- Hill, A., and K. Bloom. 1987. Genetic manipulation of centromere function. *Mol. Cell. Biol.* 7:2397–2405.
- Hill, A., and K. Bloom. 1989. Acquisition and processing of a conditional dicentric chromosome in *Saccharomyces cerevisiae*. *Mol. Cell. Biol.* 9:1368–1370.
- Hoyt, M.A., L. Totis, and B.T. Roberts. 1991. *S. cerevisiae* genes required for cell cycle arrest in response to loss of microtubule function. *Cell* 66:507–517.
- Irniger, S., S. Piatti, C. Michaelis, and K. Nasmyth. 1995. Genes involved in sister chromatid separation are needed for B-type cyclin proteolysis in budding yeast. *Cell* 81:269–278.
- Kahana, J.A., B.J. Schnapp, and P.A. Silver. 1995. Kinetics of spindle pole body separation in budding yeast. *Proc. Natl. Acad. Sci. USA.* 92:9707–9711.
- Koshland, D., L. Rutledge, M. Fitzgerald-Hayes, and L.H. Hartwell. 1987. A genetic analysis of dicentric minichromosomes in *Saccharomyces cerevisiae*. *Cell* 48:801–812.
- Levin, N.A., M.A. Bjornsti, and G.R. Fink. 1993. A novel mutation in DNA topoisomerase I of yeast causes DNA damage and RAD9-dependent cell cycle arrest. *Genetics* 133:799–814.
- Li, R., and A.W. Murray. 1991. Feedback control of mitosis in budding yeast. *Cell* 66:519–531.
- Li, X., and R.B. Nicklas. 1995. Mitotic forces control a cell-cycle checkpoint. *Nature (Lond.)* 373:630–632.
- Li, Y.Y., E. Yeh, T. Hays, and K. Bloom. 1993. Disruption of mitotic spindle orientation in a yeast dynein mutant. *Proc. Natl. Acad. Sci. USA.* 90:10096–10100.
- Lydall, D., and T. Weinert. 1995. Yeast checkpoint genes in DNA damage processing: implications for repair and arrest. *Science (Wash. DC)* 270:1488–1491.
- Murray, A. 1995a. Cyclin ubiquitination: the destructive end of mitosis. *Cell* 81:149–152.
- Murray, A.W. 1995b. The genetics of cell cycle checkpoints. *Curr. Opin. Genet. Dev.* 5:5–11.
- Nasmyth, K. 1993. Control of the yeast cell cycle by the Cdc28 protein kinase. *Curr. Opin. Cell Biol.* 5:166–179.
- Neff, M.W., and D.J. Burke. 1992. A delay in the *Saccharomyces cerevisiae* cell cycle that is induced by a dicentric chromosome and dependent upon mitotic checkpoints. *Mol. Cell. Biol.* 12:3857–3864.
- Pringle, J.R., R.A. Preston, A.E.M. Adams, T. Stearns, D.G. Drubin, B.K. Haarer, and E.W. Jones. 1989. Fluorescence microscopy methods for yeast. *Methods Cell Biol.* 31:358–435.
- Salmon, E.D., T. Inoue, A. Desai, and A.W. Murray. 1994. High resolution multimode digital imaging system for mitosis studies *in vivo* and *in vitro*. *Biol. Bull. (Woods Hole)* 187:231–232.
- Saunders, W.S., and M.A. Hoyt. 1992. Kinesin-related proteins required for structural integrity of the mitotic spindle. *Cell* 70:451–458.
- Saunders, W.S., D. Koshland, D. Eshel, I.R. Gibbons, and M.A. Hoyt. 1995. *Saccharomyces cerevisiae* kinesin- and dynein-related proteins required for anaphase chromosome segregation. *J. Cell Biol.* 128:617–624.
- Schiestl, R.H., P. Reynolds, S. Prakash, and L. Prakash. 1989. Cloning and sequence analysis of the *Saccharomyces cerevisiae* RAD9 gene and further evidence that its product is required for cell cycle arrest induced by DNA damage. *Mol. Cell. Biol.* 9:1882–1896.
- Siede, W., A.S. Friedberg, and E.C. Friedberg. 1993. RAD9-dependent G1 arrest defines a second checkpoint for damaged DNA in the cell cycle of *Saccharomyces cerevisiae*. *Proc. Natl. Acad. Sci. USA.* 90:7985–7989.
- Sigrist, S., H. Jacobs, R. Stratmann, and C.F. Lehner. 1995. Exit from mitosis is regulated by *Drosophila* fizzy and the sequential destruction of cyclins A, B, and B3. *EMBO (Eur. Mol. Biol. Organ.) J.* 14:4827–4838.
- Skibbens, R.V., V.P. Skeen, and E.D. Salmon. 1993. Directional instability of kinetochore motility during chromosome congression and segregation in mitotic newt lung cells: a push-pull mechanism. *J. Cell Biol.* 122:859–875.
- Spencer, F., and P. Hieter. 1992. Centromere DNA mutations induce a mitotic delay in *Saccharomyces cerevisiae*. *Proc. Natl. Acad. Sci. USA.* 89:8908–8912.
- Stueland, C.S., D.J. Lew, M.J. Cismowski, and S.I. Reed. 1993. Full activation of p34CDC28 histone H1 kinase activity is unable to promote entry into mitosis in checkpoint-arrested cells of the yeast *Saccharomyces cerevisiae*. *Mol. Cell. Biol.* 13:3744–3755.
- Surana, U., A. Amon, C. Dowzer, J. McGrew, B. Byers, and K. Nasmyth. 1993. Destruction of the CDC28/CLB mitotic kinase is not required for the metaphase to anaphase transition in budding yeast. *EMBO (Eur. Mol. Biol. Organ.) J.* 12:1969–1978.
- Toyn, J.H., and L.H. Johnston. 1994. The Dbf2 and Dbf20 protein kinases of budding yeast are activated after the metaphase to anaphase cell cycle transition. *EMBO (Eur. Mol. Biol. Organ.) J.* 13:1103–1113.
- Wang, Y., and D.J. Burke. 1995. Checkpoint genes required to delay cell division in response to nocodazole respond to impaired kinetochore function in the yeast *Saccharomyces cerevisiae*. *Mol. Cell. Biol.* 15:6838–6844.
- Weinert, T.A., and L.H. Hartwell. 1988. The RAD9 gene controls the cell cycle response to DNA damage in *Saccharomyces cerevisiae*. *Science (Wash. DC)* 241:317–322.
- Weinert, T., and D. Lydall. 1993. Cell cycle checkpoints, genetic instability and cancer. *Semin. Cancer Biol.* 4:129–140.
- Weinert, T.A., G.L. Kiser, and L.H. Hartwell. 1994. Mitotic checkpoint genes in budding yeast and the dependence of mitosis on DNA replication and repair. *Genes Dev.* 8:652–665.
- Wells, W.A. 1996. The spindle assembly checkpoint: aiming for a perfect mitosis, every time. *Trends Cell Biol.* 6:228–234.
- Winey, M., C.L. Mamay, E.T. O'Toole, D.N. Mastrorarde, T.H. Giddings Jr., K.L. McDonald, and J.R. McIntosh. 1995. Three-dimensional ultrastructural analysis of the *Saccharomyces cerevisiae* mitotic spindle. *J. Cell Biol.* 129:1601–1615.
- Yeh, E., R.V. Skibbens, J.W. Cheng, E.D. Salmon, and K. Bloom. 1995. Spindle dynamics and cell cycle regulation of dynein in the budding yeast, *Saccharomyces cerevisiae*. *J. Cell Biol.* 130:687–700.